$Mn_{2-x}Cr_xSb$. As pointed out by Bierstedt,[10] this transition is accompanied by hysteresis. For transitions near room temperature, the hysteresis is less than 1 deg of temperature. However, below about 200°K, hysteresis begins increasing sharply and reaches a value of about 20° for a transition occurring near the temperature of liquid nitrogen. First-order transitions to the ferromagnetic state in MnAs and the associated hysteresis have been investigated by Bean and Rodbell.[13] They point out that the maximum hysteresis arises when the spin system remains at the initial minimum of the free energy, even though it is not the lowest minimum, until the free energy is "down-hill-all-the-way." The measured hysteresis in MnAs is about 2/3 of this maximum value.

---

[13] C. P. Bean and D. S. Rodbell, Phys. Rev. 126, 104 (1962).

This situation does not hold for the F/AF transition in $Mn_{2-x}Cr_xSb$. Kittel has shown that the maximum hysteresis in a_T is $\Delta a_T = 2\rho m^2/R$. The free energy used in this treatment does not alter appreciably this expression. At room temperature, therefore, the expected hysteresis in Δa_T using ρ/R obtained previously is of the order of 10^{-2} Å, which may be transformed to a thermal hysteresis of about 50° by use of Fig. 2. This large discrepancy with the observed hysteresis indicates some very efficient mechanism nucleates the new state so that for transitions near room temperature the most stable state is nearly the equilibrium state. At low temperatures this nucleation mechanism must become less efficient, since the thermal hysteresis increases rapidly. A satisfactory model has not been obtained.

Magnetic Susceptibilities of Transition Elements in Host Crystals. II. Ni²⁺ in ZnO and CdS†

WILLIAM H. BRUMAGE AND CHUN C. LIN*

Department of Physics, University of Oklahoma, Norman, Oklahoma

(Received 10 December 1963)

The magnetic susceptibilities of Ni²⁺-doped ZnO and CdS crystals have been measured along and perpendicular to the trigonal crystalline axes over the temperature range of 28–500°K. The magnetic susceptibilities of both crystals approach constant values at low temperature and decrease more rapidly with increasing temperature at $T > 60$°K. An unusually large magnetic anisotropy is observed for Ni²⁺:ZnO. The non-Curie behavior can be explained on the basis that the ground state of Ni²⁺ is nonmagnetic (A_1) and the temperature-dependent susceptibility arises mainly from the ions in the first two excited states $(A_2$ and $E)$. By fitting the theoretical susceptibilities to the experimental values, the spin-orbit coupling constant of Ni²⁺:ZnO is obtained as -175 ± 25 cm^{-1} and the trigonal field splitting of the $T_1[^3T(F)]$ state (the lowest T_1 state) as 100 ± 10 cm^{-1}. The corresponding quantities for Ni²⁺:CdS are -170 ± 10 cm^{-1} and 10 ± 4 cm^{-1}. In both crystals the A_2 component of the $T_1[^3T(F)]$ state lies below the E level. The large reduction of the spin-orbit coupling constant from the free-ion value indicates a rather strong covalency between the Ni²⁺ ion and the ligands. Combination of the trigonal splittings of the $T_1[^3T_1(F)]$ state with those of $T_2[^3T_1(P)]$ observed in the optical spectra leads to a determination of the trigonal field parameters. The experimental values of the trigonal parameters are consistent with those calculated by using the point-charge model and assuming a local contraction of the lattice with a slightly larger contraction for the three anions off the trigonal axis than for the one on the axis.

I. INTRODUCTION

IN a previous paper we have pointed out that the magnetic susceptibilities of V³⁺-doped corundum may be used quite effectively for determining certain structural parameters of the crystals.[1] For example, the trigonal field splitting of the lowest $^3T_1$ level of V³⁺:Al₂O₃ was determined from the Van Vleck temperature-independent susceptibility which was evaluated from the magnetic data in the temperature interval of 77–295°K, and the zero-field splitting of the ground state was obtained from the susceptibilities at low tempera-

tures. By combining these results with those of electron spin resonance experiments and optical spectra,[2] the two trigonal field parameters and the spin-orbit coupling constant were estimated. The trigonal field parameters were found to be in reasonable agreement with the ones calculated from the empirical point-charge model. In this paper we shall report some magnetic measurements of Ni²⁺:CdS and Ni²⁺:ZnO. The susceptibility data make it possible to locate the first two excited states which hitherto have not been determined accurately.[3]

---

[1] W. H. Brumage, C. R. Quade, and C. C. Lin, Phys. Rev. 131, 949 (1963).

[2] D. S. McClure, J. Chem. Phys. 36, 2757 (1962).
[3] An estimation of the energy of the first excited state of Ni²⁺:ZnO has been made by intensity measurements. See R. Pappalardo, D. L. Wood, and R. C. Linares, Jr., J. Chem. Phys. 35, 1471 (1961).

Values of the spin-orbit coupling constant and the trigonal field parameters can then be obtained, and the latter are compared with the calculations of the point-charge model.

In both CdS and ZnO host crystals, a Ni²⁺ ion is situated in a tetrahedral site.[4,5] Since Ni²⁺ has an electron configuration of $(3d)^8$ and since the pattern of the energy level splitting due to a tetrahedral field is just the inverted form of that of an octahedral field, the ordering of the crystalline Stark levels of Ni²⁺:CdS and V³⁺:Al₂O₃ are identical if one ignores the effect of the trigonal distortion. However, the spin-orbit coupling constant of Ni²⁺ is considerably larger than that of V³⁺. Thus, in Ni²⁺:CdS the spin-orbit splittings are much greater than the trigonal terms, while these two effects are of comparable magnitude for Ni²⁺:ZnO. It is convenient to consider the spin-orbit interaction as the major perturbation to Ni²⁺ in a cubic field and then introduce the trigonal terms as the second perturbation. Figure 1 shows the energy level diagram of a Ni²⁺ ion in tetrahedral site.

The ground state A_1 is nonmagnetic, i.e., the average magnetic moment for this state is zero. At very low temperature the susceptibility should approach a constant value which is equal to the sum of the diamagnetism of the host crystal and the Van Vleck temperature-independent susceptibility. If we choose the trigonal axis as the z axis, it is easily shown that the matrix elements of μ_x and μ_y connect an A_1 state with only the E states, while μ_z has elements between A_1 and A_2 only. It follows that for an external magnetic field along the z axis, the Van Vleck term is dictated primarily by the first A_2 level (in the trigonal field) while in the case of a perpendicular field, the lowest E state gives the major contribution to the temperature-independent paramagnetic susceptibility. As the temperature is increased, the excited states begin to receive appreciable population and the susceptibilities then depart from the low-temperature asymptotic values. Because of this strong dependence of χ_z and χ_x on temperature, the positions of the first A_2 and the first E states can be determined quite accurately. In the case of Ni²⁺:CdS, we are able to obtain from the magnetic data a trigonal splitting of the lowest A_2-E pair as small as 10 cm⁻¹. Furthermore, since both the first excited A_2 and E levels are a few hundred cm⁻¹ above the ground state, direct determination of the location of these levels is difficult by other means and the magnetic measurements are particularly effective for this purpose.

II. EXPERIMENT

The crystals of Ni²⁺:CdS were furnished by Dr. T. L. Estle of Texas Instrument Inc., and Ni²⁺:ZnO by

[4] R. W. G. Wyckoff, *Crystal Structure* (Interscience Publishers, Inc., New York, 1948), Vol. 1; G. Heiland, E. Mollwo, and F. Stockmann, Solid State Phys. **8**, 195 (1959).
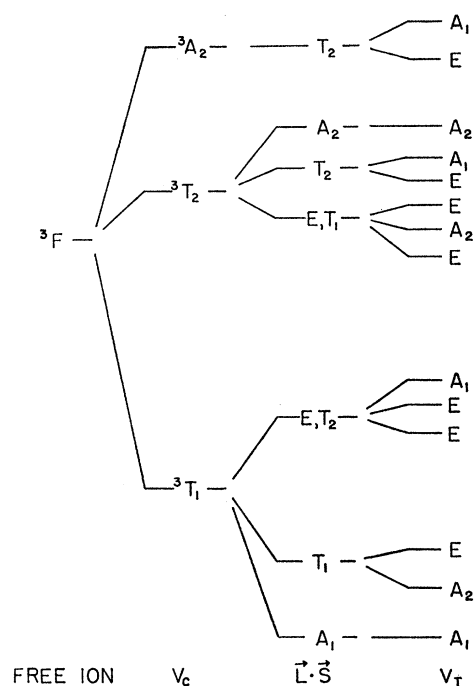[5] H. A. Weakliem, J. Chem. Phys. **36**, 2117 (1962).

Fig. 1. Energy levels (^3F) of Ni²⁺ in a trigonal field.

Dr. H. A. Weakleim of the RCA Laboratories. The measurements of the magnetic susceptibility were made by means of the Faraday balance used in our previous work.[1] In Tables I and II are shown the magnetic susceptibilities of Ni²⁺:CdS and Ni²⁺:ZnO crystals along and perpendicular to the trigonal axis over the temperature range of 28–500°K. The concentrations of the nickel ions in ZnO and CdS are 0.076 and 0.84%, respectively, as determined from the analysis of the magnetic data. The accuracy of the measured susceptibility in ZnO ($\pm4\%$) is somewhat lower than in CdS ($\pm2\%$) because of the smaller concentration of Ni²⁺ in the former.

TABLE I. Magnetic susceptibilities (per gram sample) of Ni²⁺-doped CdS crystal. Concentration: 0.84%.

T (°K)	$\chi_{\parallel}\times10^7$ (cgs-emu)	T (°K)	$\chi_{\perp}\times10^7$ (cgs-emu)
77.3	8.30	77.3	7.90
94	7.75	86	7.60
108	7.12	101	7.18
128	6.32	121	6.35
154	5.40	134	5.85
174	4.68	164	4.80
202	3.86	184	4.16
217	3.51	203	3.72
232	3.11	219	3.48
255	2.63	249	2.77
296	1.98	294	1.98
391	0.90	389	0.80
489	0.21	448	0.37

TABLE II. Magnetic susceptibilities (per gram sample) of Ni^{2+}-doped ZnO crystal. Concentration: 0.076%.

T (°K)	$x_{||}\times10^7$ (cgs-emu)	T (°K)	$x_{\perp}\times10^7$ (cgs-emu)
28.0	0.00	28.0	−1.85
77.3	−0.27	77.3	−1.85
97	−0.53	107	−1.85
108	−0.75	114	−1.95
130	−1.08	118	−2.00
140	−1.30	151	−2.10
203	−1.90	167	−2.13
253	−2.16	201	−2.35
273	−2.22	250	−2.46
300	−2.33	300	−2.57
335	−2.42	330	−2.73
403	−2.66	401	−2.86
501	−2.90	501	−2.90

III. THEORY AND ANALYSIS OF DATA

The theoretical analysis of the magnetic susceptibility of a (d^2) or (d^8) atomic system in a trigonal field has been treated in detail for the $V^{3+}:Al_2O_3$ crystals.[1] As pointed out in Sec. I, for the case of Ni^{2+} in a slightly distorted tetrahedral site, it is advantageous to consider the spin-orbit coupling as the major perturbation on the perfect tetrahedral field and the trigonal distortion as a minor one. Thus, a slight modification will be made to the theory presented in Ref. 1.

The Hamiltonian for a Ni^{2+} ion is written as

$$H=H_0+V_c+\lambda\mathbf{L}\cdot\mathbf{S}+V_t+\mu_0(\mathbf{L}+g_s\mathbf{S})\cdot\mathfrak{K}. \quad (1)$$

The various members in the right-hand side of Eq. (1) represent the Hamiltonian of a free Ni^{2+} ion, the cubic (tetrahedral) crystalline field, the spin-orbit interaction term, the trigonal field, and the interaction with the external field $\mathfrak{K}$. As was done before, the two crystal potential terms are taken as[6]

$$V_c=\sum_{i=1,2} r_i{}^4A_4{}^0\{Y_{4,0}(\theta_i\phi_i)+(10/7)^{1/2}$$
$$\times[Y_{4,3}(\theta_i\phi_i)-Y_{4,-3}(\theta_i\phi_i)]\}, \quad (2)$$

$$V_t=\sum_{i=1,2}\{r_i{}^2B_2{}^0Y_{2,0}(\theta_i\phi_i)+r_i{}^4B_4{}^0Y_{4,0}(\theta_i\phi_i)\}. \quad (3)$$

Here the summation is to be extended over the two $(3d)$ holes rather than electrons. The crystal-field parameters are defined as

$$\beta=-A_4{}^0\langle r^4\rangle/14\sqrt{\pi},$$
$$\gamma=-B_4{}^0\langle r^4\rangle/42\sqrt{\pi},$$
$$\tau=-(\sqrt{5})B_2{}^0\langle r^2\rangle/140\sqrt{\pi},$$

and, in the case of a pure cubic field β is equal to $\frac{2}{3}Dq$. Let us first consider the part of the Hamiltonian

$$H'=H_0+V_c+\lambda\mathbf{L}\cdot\mathbf{S}. \quad (4)$$

[6] See, for example, D. S. McClure, Solid State Phys. 9, 399 (1959).

The lowest configuration $(3d)^8$ of a Ni^{2+} ion gives rise to the terms ^3F, ^1D, ^3P, ^1G, and ^1S which are split by the cubic field, e.g.,

$$^3F\rightarrow{}^3T_1+{}^3T_2+{}^3A_2, \quad {}^3P\rightarrow{}^3T_1. \quad (5)$$

The spin-orbit coupling causes further splitting of the levels as

$$^3T_1\rightarrow A_1+E+T_1+T_2,$$
$$^3T_2\rightarrow A_2+E+T_1+T_2, \quad (6)$$
$$^3A_2\rightarrow T_2.$$

The eigenfunctions of H_0 corresponding to the various terms of the $(3d)^8$ configuration are taken as the usual Clebsch-Gordan type combinations[7] of one-electron orbitals, and the multiplet separations are treated as parameters to be determined from the optical spectra. From the eigenfunctions of H_0 we can construct the cubic-field functions according to Table IV of Ref. 1. These functions are characterized by the irreducible representations of the cubic group to which they belong. Since V_c has matrix elements connecting $^3T_1(^3F)$ and $^3T_1(^3P)$, a transformation

$$\begin{array}{c}^3F\\^3P\end{array}\begin{pmatrix}a_1 & a_2\\-a_2 & a_1\end{pmatrix} \quad (7)$$

must be applied to these two states in order to diago-

TABLE III. Spin-orbit functions of ^3F and ^3P.

^3F

$^3T_1$: $\phi(A_1,{}^3T_1,0)=\{\Psi(^3T_1,+,-1)-\Psi(^3T_1,0,0)+\Psi(^3T_1,-,+1)\}/\sqrt{3}$
   $\phi(T_1,{}^3T_1,0)=\{\Psi(^3T_1,+,-1)-\Psi(^3T_1,-,+1)\}/\sqrt{2}$
   $\phi(T_1,{}^3T_1,+)=\{\Psi(^3T_1,+,0)-\Psi(^3T_1,0,+1)\}/\sqrt{2}$
   $\phi(T_1,{}^3T_1,-)=\{-\Psi(^3T_1,-,0)+\Psi(^3T_1,0,-1)\}/\sqrt{2}$
   $\phi(E,{}^3T_1,+)=\{-\Psi(^3T_1,-,-1)+\Psi(^3T_1,+,0)+\Psi(^3T_1,0,+1)\}/\sqrt{3}$
   $\phi(E,{}^3T_1,-)=\{+\Psi(^3T_1,-,-1)+\Psi(^3T_1,+,0)+\Psi(^3T_1,0,+1)\}/\sqrt{3}$
   $\phi(T_2,{}^3T_1,0)=\{\Psi(^3T_1,+,-1)+2\Psi(^3T_1,0,0)+\Psi(^3T_1,-,+1)\}/\sqrt{6}$
   $\phi(T_2,{}^3T_1,+)=\{2\Psi(^3T_1,+,+1)-\Psi(^3T_1,-,0)-\Psi(^3T_1,0,-1)\}/\sqrt{6}$
   $\phi(T_2,{}^3T_1,-)=\{-2\Psi(^3T_1,-,-1)-\Psi(^3T_1,+,0)-\Psi(^3T_1,0,+1)\}/\sqrt{6}$

$^3T_2$: $\phi(A_2,{}^3T_2,0)=\{-\Psi(^3T_2,0,0)-\Psi(^3T_2,-,+1)+\Psi(^3T_2,+,-1)\}/\sqrt{3}$
   $\phi(T_2,{}^3T_2,0)=\{\Psi(^3T_2,+,-1)+\Psi(^3T_2,-,+1)\}/\sqrt{2}$
   $\phi(T_2,{}^3T_2,+)=\{\Psi(^3T_2,+,0)-\Psi(^3T_2,0,+1)\}/\sqrt{2}$
   $\phi(T_2,{}^3T_2,-)=\{\Psi(^3T_2,0,-1)+\Psi(^3T_2,-,0)\}/\sqrt{2}$
   $\phi(E,{}^3T_2,+)=\{\Psi(^3T_2,-,-1)+\Psi(^3T_2,0,+1)+\Psi(^3T_2,+,0)\}/\sqrt{3}$
   $\phi(E,{}^3T_2,-)=\{\Psi(^3T_2,+,+1)+\Psi(^3T_2,0,-1)-\Psi(^3T_2,-,0)\}/\sqrt{3}$
   $\phi(T_1,{}^3T_2,0)=\{2\Psi(^3T_2,0,0)-\Psi(^3T_2,-,+1)+\Psi(^3T_2,+,-1)\}/\sqrt{6}$
   $\phi(T_1,{}^3T_2,+)=\{2\Psi(^3T_2,+,+1)-\Psi(^3T_2,0,-1)-\Psi(^3T_2,-,0)\}/\sqrt{6}$
   $\phi(T_1,{}^3T_2,-)=\{-2\Psi(^3T_2,-,-1)-\Psi(^3T_2,0,+1)-\Psi(^3T_2,+,0)\}/\sqrt{6}$

$^3A_2$: $\phi(T_2,{}^3A_2,0)=\Psi(^3A_2,0)$
   $\phi(T_2,{}^3A_2,+)=\Psi(^3A_2,+1)$
   $\phi(T_2,{}^3A_2,-)=\Psi(^3A_2,-1)$

^3P

$^3T_1$: $\phi(A_1,{}^3T_1,0)=\{\Psi(^3T_1,+,-1)-\Psi(^3T_1,0,0)+\Psi(^3T_1,-,+1)\}/\sqrt{3}$
   $\phi(T_1,{}^3T_1,0)=\{\Psi(^3T_1,+,-1)-\Psi(^3T_1,-,+1)\}/\sqrt{2}$
   $\phi(T_1,{}^3T_1,+)=\{\Psi(^3T_1,+,0)-\Psi(^3T_1,0,+1)\}/\sqrt{2}$
   $\phi(T_1,{}^3T_1,-)=\{\Psi(^3T_1,0,-1)-\Psi(^3T_1,-,0)\}/\sqrt{2}$
   $\phi(E,{}^3T_1,+)=\{-\Psi(^3T_1,-,-1)+\Psi(^3T_1,+,0)+\Psi(^3T_1,0,+1)\}/\sqrt{3}$
   $\phi(E,{}^3T_1,-)=\{\Psi(^3T_1,+,+1)+\Psi(^3T_1,0,-1)+\Psi(^3T_1,-,0)\}/\sqrt{3}$
   $\phi(T_2,{}^3T_1,0)=\{\Psi(^3T_1,+,-1)+2\Psi(^3T_1,0,0)+\Psi(^3T_1,-,+1)\}/\sqrt{6}$
   $\phi(T_2,{}^3T_1,-)=\{-2\Psi(^3T_1,-,-1)-\Psi(^3T_1,+,0)-\Psi(^3T_1,0,1)\}/\sqrt{6}$
   $\phi(T_2,{}^3T_1,+)=\{2\Psi(^3T_1,+,+1)-\Psi(^3T_1,0,-1)-\Psi(^3T_1,-,0)\}/\sqrt{6}$

[7] E. U. Condon and G. H. Shortley, *The Theory of Atomic Spectra* (Cambridge University Press, London, 1951).

nalize H_0+V_c. This results in a mixing between the F and P states. When the spin-orbit coupling is taken into consideration, the nine functions associated with the $^3T_1$ (also $^3T_2$) must be regrouped in such a way as to exhibit the decomposition shown in (6). The symbol $\phi(T_2,{}^3T_1,+)$ is used to denote a new function obtained in this manner corresponding to the T_2 representation and originating from the $^3T_1$ state. The last symbol inside the parenthesis specifies a particular component of the degenerate state. The functions ϕ are listed in Table III. In the representation with ϕ as the basis, H' is not completely diagonal since $\mathbf{L}\cdot\mathbf{S}$ does connect members of the $^3T_1$ manifold with those of $^3T_2$.

When the trigonal field is introduced, the T_1 and T_2 split into A_2+E and A_1+E, respectively. The energy matrix (in the absence of external field) then factorizes into blocks corresponding to A_1, A_2, and E. For magnetic susceptibilities below 500°K, the highly excited states are insignificant, so we will consider only the manifold associated with the ^3F state (with F-P mixing included). The energy matrix is shown in Table IV. Any mixing of these states with higher excited states can arise only from the spin-orbit coupling or from V_t and are too small to affect the susceptibilities.

A. Ni²⁺:CdS

The optical studies reported by Weakliem[5] suggest that the environment of the Ni²⁺ in CdS is very nearly cubic because of the apparent isotropy of the spectrum. The same conclusion can also be reached from the small observed magnetic anisotropy (Table I). It is therefore convenient to diagonalize first the Hamiltonian H', defined by Eq. (3), and subsequently treat V_t by first-order perturbation. To diagonalize H' we shall take the values of β and Δ_P (the spacing between ^3F and ^3P for the limiting free ion) as 257 and 8550 cm⁻¹, respectively, according to the results of Weakliem.[5] This gives the F-P mixing coefficients as

$$a_1=0.991, \quad a_2=0.138.$$

The wave functions which diagonalize H' are now labeled by the irreducible representations of the cubic group. Thus, a wave function of a particular symmetry species can be expressed as linear combinations of the functions listed in Table III, e.g.,

$$\psi(T_2,+)=a\phi(T_2,{}^3T_1,+)+b\phi(T_2,{}^3T_2,+). \quad (8)$$

When the trigonal potential is introduced, these functions may still be used as the approximate wave function of $H'+V_t$, and the effect of V_t is to produce splittings or shifts of the energy levels. The wave functions and energies of the lowest nine states which are associated with the $^3T_1(F)$ group are determined in this manner.

With the wave functions for these nine states, the magnetic susceptibilities have been calculated by means

of the standard procedure[8] and are expressed in terms of the energy levels of the low-lying states and the matrix elements of $\mathbf{L}$ and $\mathbf{S}$ between these states. The formulas for $\chi_{||}$ and $\chi_{\perp}$ are

$$\chi_{||}=2NB\left[\frac{|(0|\mu_z|1)|^2}{\Delta_1}+\exp(-\Delta_1/kT)\right.$$

$$\times\left\{-\frac{|(0|\mu_z|1)|^2}{\Delta_1}+\frac{|(1|\mu_z|4)|^2}{\Delta_4-\Delta_1}\right\}+2\exp(-\Delta_2/kT)$$

$$\times\left\{\frac{|(2|\mu_z|2)|^2}{2kT}+\sum_{i\neq2}\frac{|(2|\mu_z|i)|^2}{\Delta_i-\Delta_2}\right\}+2\exp(-\Delta_3/kT)$$

$$\times\left\{\frac{|(3|\mu_z|3)|^2}{2kT}+\sum_{i\neq3}\frac{|(3|\mu_z|i)|^2}{\Delta_i-\Delta_3}\right\}+\exp(-\Delta_4/kT)$$

$$\times\left\{\frac{|(1|\mu_z|4)|^2}{\Delta_1-\Delta_4}\right\}+2\exp(-\Delta_5/kT)$$

$$\left.\times\left\{\frac{|(5|\mu_z|5)|^2}{2kT}+\sum_{i\neq5}\frac{|(5|\mu_z|i)|^2}{\Delta_i-\Delta_5}\right\}\right], \quad (9)$$

$$\chi_{\perp}=4NB\sum_i\left[\frac{|(0|\mu_x|i)|^2}{\Delta_i}+\exp(-\Delta_1/kT)\right.$$

$$\times\left\{\sum_i\frac{|(1|\mu_x|i)|^2}{\Delta_i-\Delta_1}\right\}+\exp(-\Delta_2/kT)$$

$$\times\left\{\frac{|(2|\mu_x|2)|^2}{2kT}+\sum_{j\neq2}\frac{|(2|\mu_x|j)|^2}{\Delta_j-\Delta_2}\right\}+\exp(-\Delta_3/kT)$$

$$\times\left\{\frac{|(3|\mu_x|3)|^2}{2kT}+\sum_{j\neq3}\frac{|(3|\mu_x|j)|^2}{\Delta_j-\Delta_2}\right\}+\exp(-\Delta_4/kT)$$

$$\times\left\{\sum_i\frac{|(4|\mu_x|i)|^2}{\Delta_i-\Delta_4}\right\}+\exp(-\Delta_5/kT)$$

$$\left.\times\left\{\frac{|(5|\mu_x|5)|^2}{2kT}+\sum_{j\neq5}\frac{|(5|\mu_x|j)|^2}{\Delta_j-\Delta_5}\right\}\right],$$

where

$$B^{-1}=1+\exp(-\Delta_1/kT)+2\exp(-\Delta_2/kT)$$
$$+2\exp(-\Delta_3/kT)+\exp(-\Delta_4/kT)+2\exp(-\Delta_5/kT),$$

and

$$i=2, 3, 5;$$
$$j=0, 1, 2, 3, 4, 5.$$

In the above equations the energy spacing between the kth level and the ground level is represented by Δ_k and the numbers 0, 1, 2, 3, 4, 5 represent the A_1, T_1A_2,

---

[8] J. H. Van Vleck, *The Theory of Electric and Magnetic Susceptibilities* (Oxford University Press, London, 1932), p. 182.

TABLE IV. Energy matrix.

A_1:

$^3T_1A\,(^3F)$	$^3T_1T_2(^3F)$	$^3T_2T_2(^3F)$	$^3A_2T_2(^3F)$	$^3T_1A\,(^3P)$	$^3T_1T_2(^3P)$
$-9\beta+3\lambda-7\gamma$	$\sqrt{2}(-10\gamma-\tau)$	$-\tfrac{1}{3}(30)^{1/2}(4\gamma-\tau)$	$-\tfrac{2}{3}(15)^{1/2}(\gamma-2\tau)$	$-6\beta-(14/3)\gamma$	$(5/3)\sqrt{2}\gamma-8\sqrt{2}\tau$
	$-9\beta-\tfrac{3}{2}\lambda+3\gamma+\tau$	$\tfrac{1}{2}(15)^{1/2}\lambda-\tfrac{1}{3}(15)^{1/2}(4\gamma-\tau)$	$-\tfrac{2}{3}(30)^{1/2}(\gamma-2\tau)$	$(5/3)\sqrt{2}\gamma-8\sqrt{2}\tau$	$-6\beta-(11/3)\gamma+(8/3)\tau$
		$3\beta-\tfrac{1}{2}\lambda-\gamma-5\tau$	$2\sqrt{2}\lambda$	$2(\tfrac{5}{6})^{1/2}(3\gamma-8\tau)$	$(5/3)^{1/2}(3\gamma-8\tau)$
			$18\beta+14\gamma$	$\sqrt{3}(4\gamma-20\tau)$	$(6)^{1/2}(-4\gamma+15\tau)$
				$\triangle_p-2\lambda$	$-14\sqrt{2}\tau$
					$\triangle_p+\lambda+14\tau$

A_2:

$^3T_1T_1(^3F)$	$^3T_2A\,(^3F)$	$^3T_2T_1(^3F)$	$^3T_1T_1(^3P)$
$-9\beta+\tfrac{3}{2}\lambda-17\gamma-\tau$	$-\tfrac{1}{3}(30)^{1/2}(4\gamma-\tau)$	$\tfrac{1}{2}(15)^{1/2}\lambda-\tfrac{1}{3}(15)^{1/2}(4\gamma-\tau)$	$-6\beta-3\gamma-8\tau$
	$3\beta-\lambda+(7/3)\gamma$	$\tfrac{1}{3}\sqrt{2}(-10\gamma-15\tau)$	$-\tfrac{1}{3}(30)^{1/2}(-3\gamma-8\tau)$
		$3\beta+\tfrac{1}{2}\lambda+(7/3)\gamma$	$-\tfrac{1}{3}(15)^{1/2}(-3\gamma-8\tau)$
			$\triangle_p-\lambda-14\tau$

E:

$^3T_1T_1(^3F)$	$^3T_1E(^3F)$	$^3T_1T_2(^3F)$	$^3T_2T_2(^3F)$	$^3T_2E(^3F)$
$-9\beta+\tfrac{3}{2}\lambda-2\gamma+\tfrac{1}{2}\tau$	$(6)^{1/2}(-5\gamma-\tfrac{1}{2}\tau)$	$+\sqrt{3}(5\gamma-\tfrac{1}{2}\tau)$	$-2(5)^{1/2}\lambda+\tfrac{1}{2}(5)^{1/2}\tau$	$-\tfrac{1}{6}(30)^{1/2}(4\gamma-\tau)$
	$-9\beta-\tfrac{3}{2}\lambda-7\gamma$	$\sqrt{2}(-5\gamma-\tfrac{1}{2}\tau)$	$\tfrac{1}{6}(30)^{1/2}(-4\gamma+\tau)$	$\tfrac{3}{2}(5)^{1/2}\lambda$
		$-9\beta-\tfrac{3}{2}\lambda-12\gamma-\tfrac{1}{2}\tau$	$\tfrac{1}{2}(15)^{1/2}\lambda+\tfrac{1}{6}(15)^{1/2}(4\gamma-\tau)$	$\tfrac{1}{2}(10)^{1/2}(4\gamma-\tau)$
			$3\beta-\tfrac{1}{2}\lambda+4\gamma+\tfrac{5}{2}\tau$	$\tfrac{1}{6}(6)^{1/2}(-10\gamma-15\tau)$
				$3\beta+\tfrac{1}{2}\lambda+(7/3)\gamma$

E:

$^3T_2T_1(^3F)$	$^3A_2T_2(^3F)$	$^3T_1T_1(^3P)$	$^3T_1E(^3P)$	$^3T_1T_2(^3P)$
$\tfrac{1}{2}(15)^{1/2}\lambda+\dfrac{(15)^{1/2}}{6}(4\gamma-\tau)$	$(10)^{1/2}(-\gamma+2\tau)$	$-6\beta-(11/2)\gamma+4\tau$	$(6)^{1/2}(-\tfrac{5}{6}\gamma-4\tau)$	$\sqrt{3}(\tfrac{5}{6}\gamma+4\tau)$
$\tfrac{1}{2}(10)^{1/2}(4\gamma-\tau)$	$\dfrac{(15)^{1/2}}{3}(2\gamma-4\tau)$	$(6)^{1/2}(-\tfrac{5}{6}\gamma-4\tau)$	$-6\beta-(14/3)\gamma$	$-\tfrac{5}{6}\sqrt{2}\gamma-4\sqrt{2}\tau$
$(5)^{1/2}(2\gamma-\tfrac{1}{2}\tau)$	$\dfrac{(30)^{1/2}}{6}(-2\gamma+4\tau)$	$\sqrt{3}(\tfrac{5}{6}\gamma+4\tau)$	$\sqrt{2}(-\tfrac{5}{6}\gamma-4\tau)$	$-6\beta+\tfrac{1}{6}\sqrt{2}(-23\gamma-24\tau)$
$\tfrac{1}{6}\sqrt{3}(10\gamma+15\tau)$	$2\sqrt{2}\lambda$	$\tfrac{1}{2}(5)^{1/2}(3\gamma+8\tau)$	$(\tfrac{5}{6})^{1/2}(3\gamma+8\tau)$	$(5/12)^{1/2}(-3\gamma-8\tau)$
$\tfrac{1}{6}\sqrt{2}(-10\gamma-15\tau)$	0	$(\tfrac{5}{6})^{1/2}(3\gamma+8\tau)$	0	$\tfrac{1}{2}(10)^{1/2}(-3\gamma-8\tau)$
$3\beta+\tfrac{1}{2}\lambda+\tfrac{2}{3}\gamma-\tfrac{5}{2}\tau$	0	$(5/12)^{1/2}(-3\gamma-8\tau)$	$\tfrac{1}{2}(10)^{1/2}(-3\gamma-8\tau)$	$\tfrac{1}{2}(5)^{1/2}(-3\gamma-8\tau)$
	$18\beta+14\gamma$	$\sqrt{2}(6\gamma-30\tau)$	$\sqrt{3}(-4\gamma+20\tau)$	$(6)^{1/2}(2\gamma-10\tau)$
		$\triangle_p-\lambda+7\tau$	$-7(6)^{1/2}\tau$	$+7\sqrt{3}\tau$
			$\triangle_p+\lambda$	$-7\sqrt{2}\tau$
				$\triangle_p+\lambda-7\tau$

T_1E, EE, T_2A_1, and T_2E levels, respectively. Here the matrix elements of $\mathbf{L}$ and $\mathbf{S}$ are to be evaluated using the wave functions of the type of Eq. (8). These elements can be written as functions of the mixing coefficients as defined in Eq. (8) which, in turn, depends on the various crystal field parameters.[9] The algebraic work, which is quite lengthy, will not be reproduced

[9] W. H. Brumage, Ph.D. thesis, University of Oklahoma, 1964 (unpublished).

here and the readers are referred to Ref. 9 for the mathematical details.

The excited states beyond the $^3T_1(F)$ manifold are at least about 3000 cm⁻¹ above the ground state, so they can be ignored as far as the magnetic susceptibility is concerned. It was found that the theoretical susceptibilities at temperatures below 500°K depend on λ and a parameter K which is defined as

$$K = -30\gamma - 3\tau, \tag{10}$$

but is practically independent of the individual values of γ and τ. The calculated susceptibilities can be fitted to the experimental data by choosing $\lambda = -170$ cm⁻¹, and $K = -20$ cm⁻¹ (see Fig. 2). These give the positions of the first two excited states (A_2 and E) as 230 and 240 cm⁻¹, respectively. It is rather remarkable to note that one is able to determine a splitting as small as 10 cm⁻¹ from the magnetic measurements. This occurs because the magnetic anisotropy depends quite sensitively on this A_2-E splitting. When the uncertainty of the experimental data is taken into consideration, the trigonal splitting is determined as 10±4 cm⁻¹. Likewise, the accuracy of λ and K is estimated to be

$$\lambda = -170 \pm 10 \text{ cm}^{-1},$$
$$K = -20 \pm 8 \text{ cm}^{-1}. \tag{11}$$

The determination of the individual values of γ and τ will be discussed in Sec. IV.

B. Ni²⁺:ZnO

The rather large magnetic anisotropy of Ni²⁺:ZnO (Fig. 3) indicates that the trigonal field here is considerably greater than that in Ni²⁺:CdS. In fact, from the susceptibility data we find that the spin-orbit coupling constant and the trigonal field parameters are of comparable magnitude. The approximate method for determining the energy levels and wave functions used in the previous section is no longer applicable here; rather one must solve the entire 21×21 secular equation as given in Table III. The amount of F-P mixing in this case is, however, quite small and can be neglected. With a given set of values of λ, γ, and τ, one can solve the secular equation numerically and calculate $\chi_{||}$ and $\chi_{\perp}$ according to Eq. (9). The wave functions for the lowest nine states are given in Ref. 9. Again the calculated susceptibilities are governed chiefly by λ and K, and by fitting the theoretical values to the experimental data, we found

$$\lambda = -175 \pm 25 \text{ cm}^{-1},$$
$$K = -225 \pm 25 \text{ cm}^{-1}. \tag{12}$$

Figure 3 shows the comparison between the theoretical and observed susceptibilities. The energies of the first two excited states (A_2 and E) are 160 and 260 cm⁻¹.
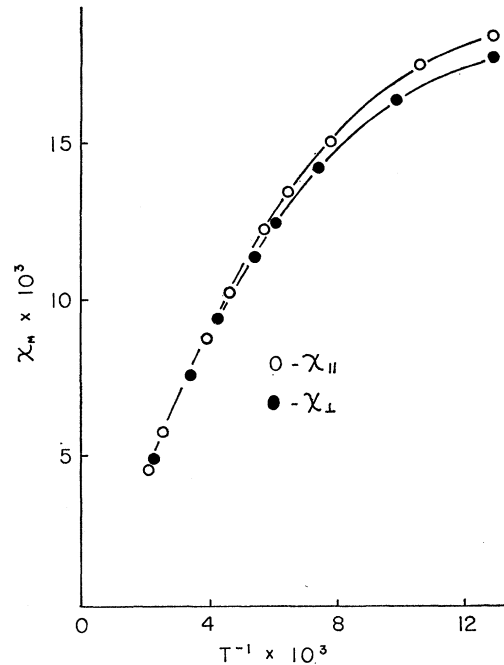

FIG. 2. Magnetic susceptibilities (per gm-ion) of Ni²⁺:CdS from 77–500°K.

IV. DISCUSSION

From the optical spectrum, Weakliem[5] has determined the trigonal splitting of the level $T_2[^3T_1(P)]$ of Ni²⁺:ZnO as 41 cm⁻¹. By combining this splitting with the parameter K given in Eq. (10), the two trigonal
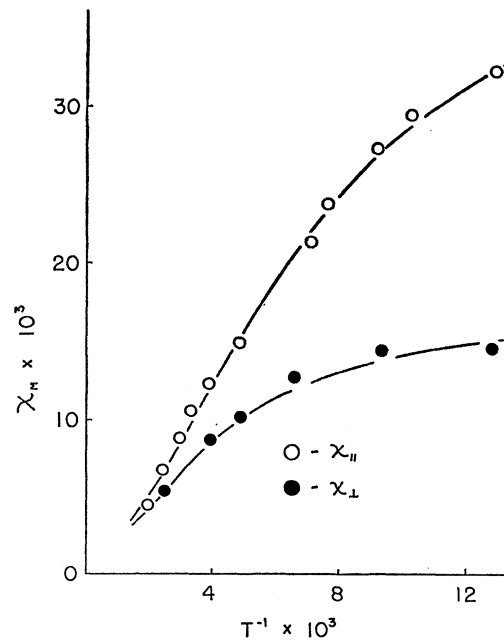

FIG. 3. Magnetic susceptibilities (per gm-ion) of Ni²⁺:ZnO from 77–500°K.

field parameters can be determined as

$$\left.\begin{array}{l}\gamma = 7.5\ \text{cm}^{-1} \\ \tau = -1.4\ \text{cm}^{-1}\end{array}\right\}, \quad \text{for Ni}^{2+}\text{:ZnO}. \qquad (13)$$

Here we found that the splitting of the $T_2[^3T_1(P)]$ state is determined primarily by τ. On the other hand, K depends mainly on γ, the contribution of τ on K being quite small. For Ni^{2+}:CdS, the trigonal splitting of $T_2[^3T_1(P)]$ was not observed in the optical spectrum, presumably too small to be resolved. In fact, the optical spectrum of Ni^{2+}:CdS shows nearly complete isotropy. If, however, it is assumed that the contribution of the τ term in K can be neglected also for Ni^{2+}:CdS, as is in the case of Ni^{2+}:ZnO, one can make an estimate of γ from K as

$$\gamma \cong 0.67\ \text{cm}^{-1}, \quad \text{for Ni}^{2+}\text{:CdS}. \qquad (14)$$

It has been shown that for the case of V^{3+}:Al$_2$O$_3$ the trigonal field parameters can be accounted for by the empirical point-charge model.[1] It is therefore interesting to make a similar analysis here. Following Ref. 1, we shall first compare the values of γ/β calculated by the point-charge model with the experimental results. The use of γ/β, rather than γ, gives a better test of the point-charge model, since the former is independent of $\langle r^4 \rangle$ as well as the effective charge assigned to the ions of the host crystals to account for the departure from purely ionic bonding. Let us first assume that the impurity ion is situated exactly at the site of Zn^{2+}. From the crystal structure data[4] and using only the four nearest-neighbor oxygen ions, we obtain from the point-charge calculation $\gamma/\beta = 0.04$ for Ni^{2+}:ZnO as compared with the experimental value of 0.027. This computation has been repeated by including in the calculation of the crystalline potential all ions of the host crystal within a radius of 20 Å from the impurity center (rather than four nearest neighbors). The ratio γ/β now becomes 0.05 which does not differ substantially from the value calculated with the nearest neighbors only. To explain the deviation of the point-charge value from experiment, we have considered the possibility of small displacement of the substituent along the trigonal axis.[1,2] The minimum value of γ/β that can be obtained by such a displacement is about 0.04. Another possible distortion is a local contraction of the lattice due to the difference in ionic radii between Ni^{2+} and Zn^{2+}. This type of distortion has been considered by several authors.[5,10] If the degree of contraction of the oxygen ion on the trigonal axis (called the unique oxygen ion) differs slightly from those of the other three, a change of γ/β will result. For example, a contraction of the three off-axis oxygen ions by 0.028 Å relative to the unique ion in the direction of the cation site will give the experimental value of $\gamma/\beta = 0.027$.

The calculation of τ from the point-charge model is considerably more difficult, as it is necessary to introduce an additional assumption of using the self-consistent field atomic wave function of Ni^{2+} to evaluate $\langle r^2 \rangle$ which is not always valid.[11] Also, the convergence of this parameter in summing over the lattice is rather poor. We have carried out the summation to 30 Å and the results still fluctuate considerably. However, we are able to obtain a rough estimate of τ as 1 cm^{-1} for the case of zero displacement of the Ni^{2+} from the cation site and no distortion of the lattice. With the distorted lattice as used in the previous paragraph (and no displacement of the impurity ions), the value of τ becomes -7 cm^{-1} which is of the same sign as the experimental value. In view of the assumptions involved in the calculation of τ, it is not reasonable to expect anything more than a qualitative agreement with experiment, and thus the point-charge calculation of this parameter will not be pursued further at this stage.

In the case of Ni^{2+}:CdS, the point-charge model gives, for zero displacement and no distortion, $\gamma/\beta = 0.018$ which is much larger than the experimental value. We have used only the nearest-neighbor anions for this calculation since the inclusion of ions at lattice sites further away, as we have seen earlier, will not change this parameter greatly. From the apparent isotropy of the optical spectrum[5] as well as the smallness of γ/β, we note that the crystalline field around the Ni^{2+} in CdS has considerably smaller trigonal components than is inferred from the crystal structure of CdS. Like the case of Ni^{2+}:ZnO, the experimental value of γ/β cannot be explained by the displacement of the substituent alone. On the other hand, the picture of local distortion where the lattice relaxes toward the impurity ion in such a manner as to restore back to a nearly perfect tetrahedral configuration, does account for the small apparent anisotropy. Indeed, the experimental value of γ/β corresponds to a contraction of the three off-axis anions through 0.02 Å relative to the fourth one. The idea of local lattice contraction in Ni^{2+}:CdS was suggested by Weakliem in his optical studies.[5]

Thus, in both Ni^{2+}:ZnO and Ni^{2+}:CdS, the experimental values of the trigonal field parameters are consistent with those calculated from the empirical point-charge model[1] with a local distortion of the lattice such that the three anions of the trigonal axis relax toward the Ni^{2+} slightly more than does the one on the axis. Of course, the point-charge model is a highly idealized picture. When it is applied to crystals with an appreciable amount of covalency, a "displacement" of the anion may result from an actual movement of the lattice site as well as a shift of the electron cloud due to a change of the degree of covalency. In our application here no sharp distinction can be made between these two effects and the term "lattice distortion" really

[10] R. S. Title, Phys. Rev. **131**, 2503 (1963).

[11] D. S. McClure, J. Chem. Phys. **38**, 2289 (1963).

refers to a movement of the effective center of charge of the anion.

The spin-orbit coupling constants of Ni^{2+} in both CdS and ZnO are about one-half of the free-ion value (-340 cm^{-1}). They are also substantially smaller than the spin-orbit constants of Ni^{2+} in octahedral field, e.g., -245 cm^{-1} for Ni^{2+}:MgO,[12] and -250 cm^{-1} (or -270) for Ni Tutton salt.[12] Similar reduction from the free-ion values was also found for the Slater-Condon parameters for Ni^{2+} in CdS and ZnO from the analysis of the optical spectra.[5] These results point toward the idea of strong bonding between the impurity ion and the ligands. One also notices the fact that the Slater-Condon parameters are appreciably smaller for Ni^{2+} in CdS than in ZnO which is suggestive of a stronger covalency in the former. However, the same sort of difference in λ(-170 ± 10 cm^{-1} versus -175 ± 25 cm^{-1}) is not so obvious from the magnetic measurements, although a larger covalency in Ni^{2+}:CdS is compatible with our results within their limits of accuracy. It is interesting to note that a substantially larger reduction of the spin-orbit constant has been reported in Cu^{2+}:ZnO.[13]

Our analysis leads to the conclusion that the magnetic susceptibilities of Ni^{2+} in CdS and ZnO can be explained quantitatively by using the ligand field theory. The considerable reduction of the spin-orbit coupling constant indicates delocalization of the valence electrons of the Ni^{2+}. It has been pointed out that even in the case of Cu^{2+}:ZnO where an unusually strong bonding beetween the impurity ions and the ligands is found, the delocalized electrons in Cu^{2+}:ZnO extend only over the Cu^{2+} ion and its nearest neighbors.[13] Thus the use of the ligand field theory in our case should be justifiable. The effect of the covalent bonding is taken into account by making the spin-orbit constant an adjustable parameter. In fact, if one assumes different degrees of covalency between the one-electron orbitals t_2 and e as was done for Cu^{2+}:ZnO, the spin-orbit interaction is then described by two parameters, i.e., $(t_2|H_{s-0}|t_2)$ and $(t_2|H_{s-0}|e)$. However, since at $T<500°$K the magnetic susceptibility is governed primarily by the ground state and the two trigonal components of $T_1[^3T_1(F)]$, and since all these two states belong to the $(t_2)^2$ configuration

(in the notation of the strong-field scheme), the susceptibility should be rather insensitive to $(t_2|H_{s-0}|e)$ and hence the value of λ determined here corresponds to the coupling constant of the t_2 state. It has also been customary to introduce an additional parameter, the "orbital reduction factor" k, which relates the matrix elements of the orbital angular momentum evaluated by using the ligand field LCAO MO with those evaluated by the pure atomic functions.[13,14] Generally, this factor is not much less than one even when there is a considerable reduction in λ. For instance, in the case of Fe^{2+} in ZnF_2,[15] the spin-orbit constant is about 60% of the free-ion value and k is around 0.95. Even in the very strong bonding case of Cu^{2+}:ZnO where λ is less than 10% of the value of a free Cu^{2+}, the orbital reduction factor is only 0.46.[13] In our theoretical analysis here, this reduction ratio is not used, i.e., it is taken as unity. When the orbital reduction ratio is included in the theory, all the matrix elements of $\mathbf{u}$ which are relevant in the calculation of the susceptibility, are modified by the same multiplicative constant. The inclusion of k merely alters the theoretical χ by a constant factor and has the same effect as changing the concentration of the nickel ion. Thus the orbital reduction ratio cannot be obtained from our susceptibility data as the precise concentrations of Ni^{2+} in both ZnO and CdS are not known. On the other hand, the crystal field parameters λ and K affect the shape of the curve of χ versus T rather than the absolute magnitude of the susceptibility, hence the values of these parameters which we gave in the preceding paragraphs still stand correct even when the orbital reduction factor is taken into consideration.

[12] W. Low, Phys. Rev. **109**, 247 (1948); J. H. E. Griffiths and J. Owen, Proc. Roy. Soc. (London) **A213**, 459 (1952).

[13] R. E. Dietz, H. Kamimura, M. D. Sturge, and A. Yariv, Phys. Rev. **132**, 1554 (1963).

[14] W. Low, in *Solid State Physics*, Suppl. 2, edited by F. Seitz and D. Turnbull (Academic Press Inc., New York, 1960), pp. 99, 100.

[15] M. Tinkham, Proc. Roy. Soc. (London) **A236**, 549 (1956).